CHEMISTRY
A EUROPEAN JOURNAL

DOI: 10.1002/chem.200903519

Cyclodextrin-Based Bimodal Fluorescence/MRI Contrast Agents: An Efficient Approach to Cellular Imaging

Zuzana Kotková,[a] Jan Kotek,*[a] Daniel Jirák,[b] Pavla Jendelová,[c] Vít Herynek,[b] Zuzana Berková,[d] Petr Hermann,[a] and Ivan Lukeš[a]

Abstract: A novel bimodal fluorescence/MRI probe based on a cyclodextrin scaffold has been synthesized and characterized. The final agent employs the fluorescein (F) functionality as a fluorescence marker and the Gd^{III} complex of a macrocyclic DOTA-based ligand (GdL) having one aminobenzylphosphinic acid pendant arm as an MRI probe, and has a statistical composition of $(GdL)_{6.9}$-$F_{0.1}$-β-CD. Slow rotational dynamics (governed by a very rigid cyclodextrin scaffold) combined with fast water exchange (ensured by the chosen macrocyclic ligand) resulted in a high relaxivity of $\sim 22\ s^{-1}\,mM^{-1}$ per Gd^{III} or $\sim 150\ s^{-1}\,mM^{-1}$ per molecule of the final conjugate (20 MHz, 25 °C). In vitro labelling of pancreatic islets (PIs) and rat mesenchymal stem cells has been successfully performed. The agent is not cytotoxic and is easily internalized into cells. The labelled cells can be visualized by MRI, as proved by the detection of individual labelled PIs. A fluorescence study performed on mesenchymal stem cells showed that the agent stays in the intracellular space for a long time.

Keywords: cell tracking · contrast agents · gadolinium · imaging agents · magnetic resonance imaging

Introduction

Modern medicine has been evolving rapidly during the last few decades. Nowadays, physicians utilize various diagnostic techniques to detect diseases or to follow processes in the human body. One of the most universal methods is magnetic resonance imaging (MRI), which is used to visualize the internal structure and function of the body. MRI provides much greater contrast between the different soft tissues of the body than computed tomography (CT), making it especially useful in neurological (brain), musculoskeletal, cardiovascular, and oncologic imaging. Recently, advances in MRI have extended its application from routine clinical diagnosis to in vivo cellular imaging.[1]

Image contrast is often increased by the administration of contrast agents (CAs) and, in some special applications (e.g., cell imaging), it is useful to apply combined (bimodal or dual) CAs, which allow imaging by two different methods depending on the particular situation.

In the field of MRI, contrast agents can be divided into two principal groups, based on the mechanism of their action. Complexes of paramagnetic ions such as Gd^{III} or Mn^{II} efficiently facilitate proton longitudinal relaxation and, thus, they are commonly called "T_1" or "positive" agents, as they increase signal intensity. On the contrary, nanocrystalline ferromagnetic phases (usually iron oxides, generally called SPIO, SuperParamagnetic Iron Oxide) affect mainly transverse relaxation, and are called "T_2" or "negative" CAs, as they decrease signal intensity. In clinical practice, "positive" CAs based on Gd^{III} complexes are of primary importance. These compounds commonly incorporate polydentate ligands based on both linear and macrocyclic poly-

[a] Dr. Z. Kotková, Dr. J. Kotek, Dr. P. Hermann, Prof. I. Lukeš
Department of Inorganic Chemistry, Univerzita Karlova v Praze
(Charles University in Prague), Hlavova 2030
128 40 Praha 2 (Czech Republic)
Fax: (+420) 22195-1253
E-mail: modrej@natur.cuni.cz

[b] Dr. D. Jirák, Dr. V. Herynek
MR Spectroscopy, MR Unit, Department of Diagnostic
and Interventional Radiology
Institute for Clinical and Experimental Medicine
Vídeňská 1958, 140 21 Praha 4 (Czech Republic)

[c] Dr. P. Jendelová
Department of Neuroscience, Institute of Experimental Medicine
ASCR
v.v.i., Vídeňská 1083, 142 20 Praha 4 (Czech Republic)

[d] Dr. Z. Berková
Laboratory of Pancreatic Islets
Institute for Clinical and Experimental Medicine
Vídeňská 1958, 140 21 Praha 4 (Czech Republic)

Supporting information for this article is available on the WWW under http://dx.doi.org/10.1002/chem.200903519.

amines bearing acetate pendant arms (DTPA and DOTA; Figure 1).[2,3]

The efficiencies of these clinically used T_1 CAs, expressed by their relaxivity r_1, are very low, but theory predicts that much higher effectiveness might be achieved by tuning the

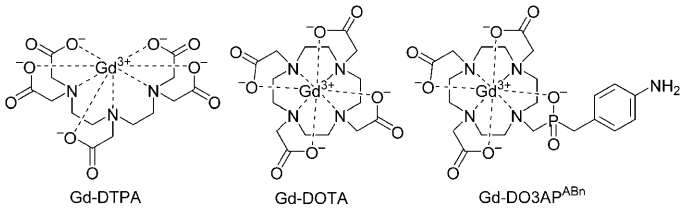

Figure 1. Some of the compounds mentioned in the text. The water molecules coordinated to Gd^{III} ions are omitted for the sake of clarity.

physico-chemical characteristics of the CAs, mainly the rotational correlation time of the whole molecule (τ_R). In addition, a change in the residence time of the water molecule(s) coordinated to the central Gd^{III} ion (τ_M) may also lead to some increase in the relaxivity.[2] In general, clinically used CAs display exchange rates that are too slow (long τ_M) and rotation that is too fast (short τ_R) due to their low molecular weights.[4] However, it was shown that the water-exchange rate is close to optimal for derivatives of DTPA or DOTA having one phosphorous acid pendant arm.[5] The rotational time should be as long as possible for lower-field scanners (<1.5 T), but it has been suggested that medium-molecular-weight compounds should yield the highest efficiencies for high-field scanners (>3 T).[6] The rotational time may be extended by conjugation of the chelate to a macromolecule, for example, a dendrimer.[7] However, it has been proved that the dangling arms of such macromolecules are too mobile, effectively cancelling out the benefit obtained by increasing the molecular volume/weight of the CAs.[8] Thus, low flexibility of the core, a rigid spacer, and a medium-molecular-weight size of the whole molecule are required, especially for CAs suitable for MRI at the higher fields[6] that are utilized in modern medical/molecular biology laboratories and clinics.

Loading cell cultures with suitable CAs offers the possibility of tracking the cells after transplantation and studying their fate in the recipient organism.[9] For work with in vitro cell cultures, standard microscopic techniques are still the most convenient; however, the common MRI CAs taken up by cells cannot be visualized directly. Therefore, bimodal probes are useful,[10] that is to say, those with combined luminescent/MRI functionalities.[11] For this reason, a mixture of isostructural lanthanide (Eu^{III}/Gd^{III}) complexes has been used in cellular labelling.[12] A Gd–DTPA complex with a fluorescent agent has also been used for the investigation of stem cells.[13] However, for Gd-based CAs, macrocyclic chelates (DOTA-like) are preferable to open-chain ones (DTPA-like), as the latter show much lower kinetic stability under in vivo conditions.[14] Therefore, Gd–DOTA derivatives with fluorescent units,[15] Gd–DOTA-modified Q-dots[16] or Au nanoparticles,[17] a lipidic rhodamine derivative,[18] and Gd–DOTA/fluorescein-labelled peptides[19] have been studied. Alternatively, some bimodal T_2-CAs have been prepared and tested, for example, fluorescein-labelled iron(III) oxide nanoparticles, and these have been used for in vivo studies of pancreatic islets (Langerhans islets, PI).[20] However, for practical reasons, T_1-CAs are more suitable for cellular imaging as they produce positive contrast.

We decided to employ a rigid core of cyclodextrin[21] to prepare T_1-CAs showing a high relaxivity and containing a suitable fluorescent label to enable the direct observation of the uptake process. Attention has been paid to the careful design of the CA to allow the simultaneous optimization of the parameters crucial for MRI and cell labelling. Optimal τ_M (<50 ns) and kinetic inertness were guaranteed by using a macrocyclic ligand moiety with one phosphorous acid pendant arm, $DO3AP^{ABn}$ (Figure 1),[5b,22] and optimal τ_R was expected after the conjugation[8e] of several ligand molecules to a rigid per-6-amino-β-cyclodextrin core through thiourea bridges. The cyclodextrins are known to exhibit wide biocompatibility and negligible toxicity and, thus, suitability for cell labelling. Bimodality of the overall conjugate was achieved by the attachment of a fluorescein molecule (through isothiocyanate coupling); the fluorescein dye is well-established and one of the most commonly used fluorescent labels. This new bimodal medium-sized contrast agent, exhibiting a high relaxivity confined to a small molecular space, has been used for the imaging of PIs and stem cells.

Results and Discussion

Synthesis: Per-6-amino-β-cyclodextrin was prepared according to the published procedure.[23] A fluorescein-labelled cyclodextrin core was prepared by the reaction of $(NH_2)_7$-β-CD with two molar equivalents of fluorescein isothiocyanate (FITC)[24] in DMSO (Scheme 1). Residual low-molecular-weight fluorescein-based compounds were removed by ultrafiltration through a 1 kDa filter in water. We assume that the fluorescence of the product was caused by fluorescein molecules covalently attached to the cyclodextrin core rather than by those non-covalently bonded within the cyclodextrin cavity as the volume of water used for ultrafiltration was enormous (around 500 mL per ultrafiltration), which should have removed all guests from the generally weak non-covalent host–guest complexes. The expected close to 2:1 fluorescein-to-cyclodextrin ratio was confirmed by ^{1}H NMR signal integration (see Figure S1) and by comparing the intensity of UV/Vis absorption (product solution vs. ultrafiltration waste), which showed less than 10% loss of the fluorescein label.

Based on this assumption, one can suggest that a statistical mixture containing predominantly singly- and doubly-substituted aminocyclodextrin cores was obtained, with small amounts of unsubstituted and triply- and more highly substituted cyclodextrins. To confirm this hypothesis, we acquired mass spectra (although these results have to be treat-

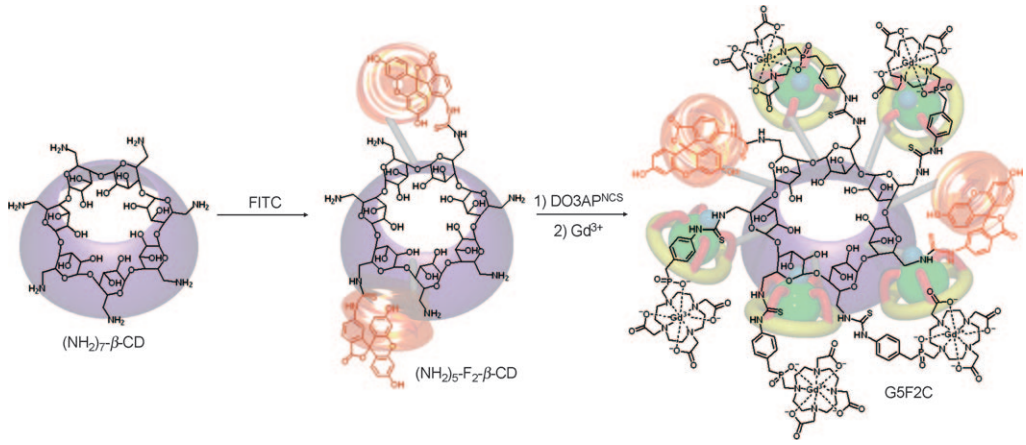

Scheme 1. Synthesis of the G5F2C bimodal contrast agent. The water molecules coordinated to Gd^{III} ions are omitted for the sake of clarity.

ed with caution as mass spectrometry is not a quantitative method due to principally different ionization abilities of even structurally related compounds). The mass spectra of the isolated conjugates dissolved in H_2O/MeOH mixtures were rather noisy with no noticeably strong signals. The spectral quality significantly increased when a small amount of trifluoroacetic acid was added to the sample. In the ESI mass spectra acquired in negative mode, the molecular peaks of the singly- and doubly-labelled cyclodextrins [$(NH_2)_6$-F-β-CD and $(NH_2)_5$-F_2-β-CD, respectively] were the most intense features (Figure S2C, Table S1), and no signal due to the starting $(NH_2)_7$-β-CD was detected, despite the fact that mass spectra of the pure starting cyclodextrin show intense molecular peaks in both the positive and negative modes (Figure S2 (A, B); Table S1). Upon addition of one weight equivalent of starting per-6-amino-β-cyclodextrin to the sample of the conjugate, signals attributable to the unsubstituted aminocyclodextrin appeared, with comparable intensities to those of $(NH_2)_6$-F-β-CD and $(NH_2)_5$-F_2-β-CD (Figure S2D, Table S1). The situation is slightly different in the positive mode: in the spectra of the conjugation products, signals attributable to $(NH_2)_6$-F-β-CD and $(NH_2)_5$-F_2-β-CD as well as that of the sodium adduct of the starting $(NH_2)_7$-β-CD are present; however, the most intense peak ($m/z \approx 1523$), which is very close to the signal of $(NH_2)_6$-F-β-CD ($m/z \approx 1518$), could not be identified (Figure S2E, Table S1). Although fragmentation of the ion with m/z 1518 [$(NH_2)_6$-F-β-CD] gives only a signal attributable to cyclodextrin (1128.7; calcd. 1128.5 for $[M+H]^+$), the fragmentation spectrum of the m/z 1523 ion is rather more complicated (Figure S2 (F,G)).

In conclusion, mass spectrometry confirmed the presence of $(NH_2)_6$-F-β-CD and $(NH_2)_5$-F_2-β-CD species in the product mixture, but the presence of unreacted $(NH_2)_7$-β-CD could not be fully excluded. Although this species was not found in the negative-mode spectra (but was detectable under the conditions employed as its signals appeared when the compound was added to the sample), it was detected as its sodium adduct in the positive-mode spectra (however, no other compound formed detectable sodium adducts, which suggests that the Na^I–CD adduct is probably extremely stable and can lead to overestimation of the amount of cyclodextrin in the mixture). In addition, as almost two whole equivalents of FITC underwent the conjugation reaction (see above), one can infer that free aminocyclodextrin is likely to be present in the final product mixture only in trace amounts. In the following text, the label $(NH_2)_5$-F_2-β-CD refers to the crude mixture of all these species obtained from FITC–CD conjugation in a 2:1 ratio.

The choice of DMSO as the solvent for FITC-$(NH_2)_7$-β-CD conjugation is crucial to achieve a high conversion; reactions in other tested solvents (pure ethanol, ethanol/water, and DMSO/water mixtures) led to very poor labelling due to low solubility of the starting materials in these media. In these cases, more than 95% of the absorption intensity was washed out from the reaction mixture, and ultrafiltration afforded material with a fluorescein-to-cyclodextrin ratio of <0.1:1. Although the presence of the fluorescent probe was obvious as the material was still highly coloured, signals corresponding to fluorescein were barely detectable in the ^1H NMR spectra and could not be reasonably integrated due to their broadness. In the ESI mass spectra, the major peak of the parent $(NH_2)_7$-β-CD was found. Although the fluorescence intensity of such material is sufficient for cellular labelling, the material cannot be reliably chemically or spectroscopically characterized. More conveniently, this material with a 0.1:1 fluorescein-to-cyclodextrin ratio was alternatively obtained using DMSO as the solvent, using only a 0.1:1 ratio of the starting FITC and $(NH_2)_7$-β-CD, indicating that this solvent allows the preparation of a CD core with any chosen amount of label.

The macrocyclic isothiocyanate derivative $DO3AP^{NCS}$[25] was conjugated to the labelled cyclodextrin core $(NH_2)_5$-F_2-β-CD in a stepwise manner (using a 100% overall excess of $DO3AP^{NCS}$ per free amino group) at pH ≈ 8 (Scheme 1). This procedure minimizes the undesired hydrolysis of the NCS group of $DO3AP^{NCS}$ to an amino group and the formation of a ditopic derivative with two macrocyclic rings con-

nected via a thiourea bridge.[25] The pure conjugate was obtained by ultrafiltration using a 3 kDa cut-off membrane, which removed the hydrolyzed by-product and the ditopic derivative.[25] The load of the chelate was determined by ^{1}H NMR signal integration (Figure S1) and by elemental analysis using the C/P/N/S ratio, which is independent of the water and counter-ion content in the solid samples. However, mass spectrometric characterization of the conjugate failed due to the high charge on the product molecule. The Gd^{III} complex was prepared by mixing a solution of the conjugate L_5-F_2-β-CD with a large (50%) excess of $GdCl_3 \cdot 6H_2O$. Free Gd^{III} ions were then complexed by the addition of an excess of Na_2H_2EDTA (1 equiv with respect to the total amount of Gd^{III}), and all low-molecular-weight impurities were removed by ultrafiltration (3 kDa), yielding the final agent $(GdL)_5$-F_2-β-CD (G5F2C; Scheme 1). It was found that the fluorescence properties of the fluorescein label in the final conjugate G5F2C ($\lambda_{em,max} = 532$ nm) were not altered, neither due to the presence of the Gd^{III} complex molecules nor due to the possibility of close contacts between neighbouring fluorescein labels, as can be seen from a comparison of the spectrum of G5F2C with those of fluorescein and fluoresceinamine itself ($\lambda_{em,max} = 529$ and 518 nm, respectively; see Figure S3). Mass spectrometric characterization of the final agent failed, probably due to the high charge on the molecule and the isotopic pattern of gadolinium. As the high fluorescein content in the molecule results in higher toxicity (see below), the whole reaction sequence was repeated using cyclodextrin labelled with 0.1 equiv of fluorescein, yielding a contrast agent with the formula $(GdL)_{6.9}$-$F_{0.1}$-β-CD (i.e., statistically, one-tenth of the cyclodextrin is derivatized by one fluorescein label); this material is referred to as G6.9F0.1C in the following text and was used in most of the studies. As the fluorescein fragment is well known to undergo photo-bleaching after extensive irradiation (e.g., in fluorescence microscopy), the agent G5F2C (with a higher content of fluorescein) was employed in those applications requiring repeated irradiation of the same area, especially for studying the persistence of the new agent in cells; in the following text, the general label GFC is used for both studied compounds.

The ligand used in the G5F2C agent was fully chemically characterized. Even though the ^{1}H NMR signals are broad and the number of protons belonging to the fluorescent label is very low compared to those responsible for the other signals, integration of the spectra afforded consistent and reliable results (see Figure S1). The ligand used in the G6.9F0.1C agent could not be characterized due to its broad NMR signals, which prevent reliable interpretation of the spectra and, in particular, do not permit determination of the fluorescent dye content. However, the agent G6.9F0.1C is expected to be useful for MRI tracking of implanted cells due to its higher Gd^{III} content, yielding a higher relaxivity per molecule of the probe.

The relaxivity (r_1) of the new contrast agent G6.9F0.1C was found to be very high, reaching a value of 22 $s^{-1}mM^{-1}$ (i.e., ~150 $s^{-1}mM^{-1}$ per molecule of CA; 20 MHz, 25°C; Table 1). The density of the relaxivity (relaxivity recalculated per molecular weight)[26] is 24 $s^{-1}g^{-1}dm^3$, which is much higher than those of simple Gd^{III} chelates, and higher than the density of relaxivity of dendrimeric Gd–DO3AP^{ABn}–PAMAM conjugates (the 1st (Figure S4) and 4th generations, $G8G^1$ and $G59G^4$, respectively, having the same complex unit; Table 1).[8a] Although it is lower than the density of relaxivity reported for several self-assembled metallostars (reaching values of about ~43 $s^{-1}g^{-1}dm^3$ at 25°C and 20 MHz; for a representative structure, see Figure S4),[6,26,27] in those cases, kinetically unstable chelates not suitable for cellular labelling[6,14,28] with two directly coordinated water molecules were used. The relaxivity of the GFC is much higher than those of the previously reported cyclodextrin-based CAs.[21]

Table 1. Relaxivity r_1 [$s^{-1}mM^{-1}$] and the density of relaxivity $\rho(r_1)$ [$s^{-1}g^{-1}dm^3$] of the newly synthesized CAs and their comparison with those of related molecules (20 MHz, 25°C).

	G6.9F0.1C	$G8G^1$/$G59G^4$[a]	Gd–DO3AP^{ABn}[b]	Gd–DOTA[c]
r_1	21.6	14.8/25.8	5.7	3.8
$\rho(r_1)$	24	16.4/12.8	8.3	6.7

[a] Ref. [8a]. [b] Ref. [5b]. [c] Ref. [4].

It was proved that the GFC agents also have a high relaxivity at high imaging fields. The relaxivity reaches 12.1 $s^{-1}mM^{-1}$ (per Gd^{III} centre, that is, about 60–80 $s^{-1}mM^{-1}$ per molecule) at 4.7 T (200 MHz) and 25°C, compared to the relaxivity of 3.6 $s^{-1}mM^{-1}$ measured for Gd–DOTA under the same conditions. Figure 2a shows an MR image acquired at 4.7 T of GFC and Gd–DOTA solutions (concentration range 0.1–2 mM) sealed in 1 mm capillaries; the new agent shows about fourfold higher efficiency. At higher concentrations, a significant decrease in signal intensity was observed due to a large T_2 effect (see Figure S5).

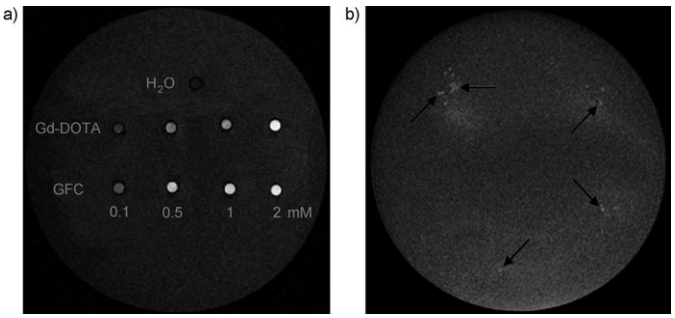

Figure 2. a) Comparison of MRI phantoms (4.7 T, 25°C) of water (top), Gd–DOTA (upper line), and GFC (lower line). Concentrations of the samples (from left to right): 0.1, 0.5, 1, and 2 mM of Gd^{III}, well diameter 35 mm. b) MRI visualization (4.7 T, 25°C) of pancreatic islets labelled by G6.9F0.1C. Arrows show areas where islets are present. Labelling conditions: 1 mM of Gd^{III} (in G6.9F0.1C), 37°C, 24 h. Well diameter 35 mm.

Labelling of pancreatic islets: The prepared bimodal contrast agent was used for imaging pancreatic islets (islets of Langerhans) or stem cells. Pancreatic islets (PIs) are clusters

of cells, present in the pancreas, which are responsible for the production of several hormones, including the most important one, insulin. Nowadays, a very promising approach to the treatment of type 1 diabetes mellitus appears to be the transplantation of PIs into the liver.[29] Therefore, the tracking of PIs is one of the major topics in cellular imaging.[30] They have been labelled using MRI CAs based on simple Gd^{III} chelates[31] or SPIO particles.[32] PIs efficiently accumulate even low-molecular-weight Gd-based CAs with a low efflux;[31] nevertheless, as PIs consists of several types of cells and only an MRI-active CA was used in this case, it was not possible to precisely localize the CA inside the islets. For this reason, we chose the new dual CA for the labelling of PIs.

After transplantation, the islets were followed exclusively by MRI; therefore, a phantom study of labelled islets was performed first. This study revealed that the uptake of CA by pancreatic islets was sufficient to visualize individual islets by MRI. Figure 2b shows an MRI scan of a gelatine phantom with dispersed pancreatic islets. Under analogous conditions, non-labelled islets produced inferior contrast (Figure S6).

As mentioned above, pancreatic (Langerhans) islets consist of several types of cells. They are mainly α-cells (~20%, producing glucagon) and β-cells (the most abundant type, ~70%, responsible for insulin production). In addition, several other cell types are present in low abundances, including those producing other hormones (e.g., somatostatin) and macrophages. To investigate which types of cells actively take up the CA (or to assess whether the CA was present only in the intercellular space of the PI), we acquired fluorescent photomicrographs. The results are presented in Figure 3. Figure 3a shows the distribution of the G6.9F0.1C agent (green) overlaid with a visualization of karyons using standard 4′,6-diamidino-2-phenylindole (DAPI) labelling (blue). It can be seen that G6.9F0.1C was taken up by macrophages, α-cells, and β-cells, as indicated by the selective co-labelling of these types of cells shown in Figure 3b–d.

Insulin secretion by the labelled PIs was studied by static incubation in media with low (3.3 mM) and high (22 mM) glucose levels. This revealed that insulin production was not altered by the labelling of the islets. In addition, the total viability of the cells forming PIs was found to be ~85–90%, showing negligible toxicity of the new CA.

Labelling of stem cells: Another topic of interest involving cell tracking is the imaging of stem cells, as cell therapies using the transplantation of such cells are very promising, especially in neurosurgery, cardiology, and the treatment of ischemic limb disease.[33] In these cases, nanocrystalline T_2 SPIO CAs have usually been used,[34] although Gd-based CAs have also been utilized.[13,35] As a model for testing the suitability of our bimodal GFC, we have chosen rat mesenchymal stem cells (rMSCs) as an example of adult stem cells, since they are easily derived from bone marrow, can differentiate into a variety of specialized cell populations, and are efficiently proliferated in vitro.

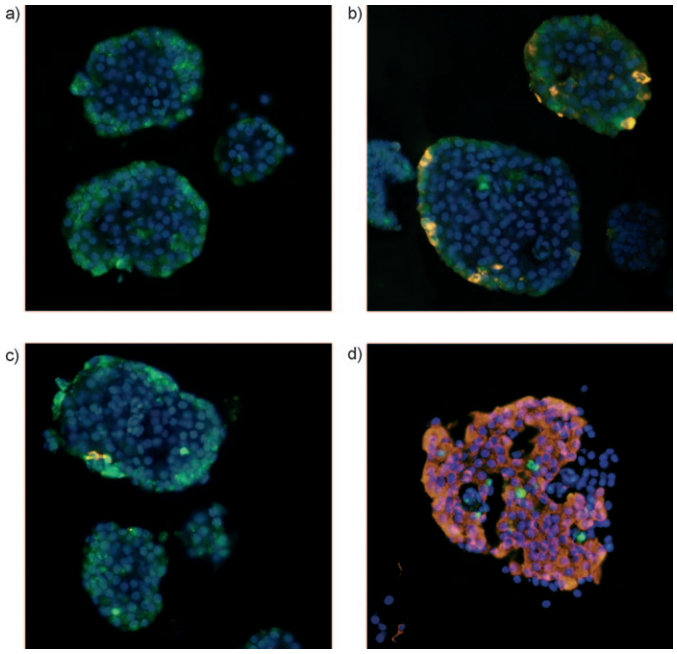

Figure 3. Fluorescent photomicrographs of sliced pancreatic islets labelled by G6.9F0.1C: a) visualization of the contrast agent (green) and karyons (blue); b) immunodetection of the α-cells by antibody conjugated with Alexa Fluor 555 (orange) merged with immunofluorescence of the contrast agent (green); c) immunodetection of the macrophages (Alexa Fluor 555, orange) merged with immunofluorescence of the contrast agent (green); d) immunodetection of the β-cells (Alexa Fluor 555, orange) merged with immunofluorescence of the contrast agent (green). Islets were incubated with 1 mM G6.9F0.1C (per Gd^{III}) at 37°C for 24 h. The size of pancreatic islets is in the range 50–450 μm.

The cells were labelled by cultivation for 48 h in media containing G6.9F0.1C agent with 1–8 mM Gd^{III}. The cells were harvested and washed, and their suspensions were transferred into capillaries, where they were left to settle. A T_1-weighted MRI slice through the settled cells showed a noticeable contrast between suspensions of the labelled and the control cells. Even the lowest concentration used (1 mM) was sufficient for significant highlighting of the suspended cells (Figure 4).

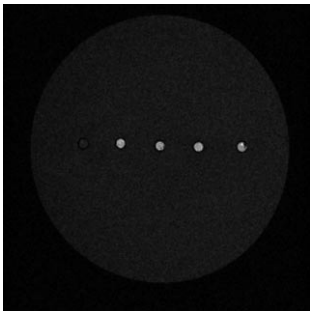

Figure 4. MRI visualization of stem cells labelled by G6.9F0.1C. Isolated stem cells (~10^6) were placed in 1 mm thick capillaries, which were then sealed. The cells were left to settle by gravity. Conditions of labelling (from left to right): control experiment, 1, 2, 4, and 8 mM of G6.9F0.1C per Gd^{III}, 37°C, 48 h. Well diameter 35 mm.

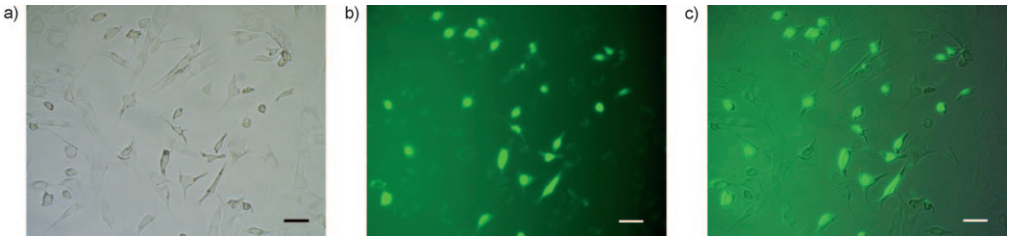

Figure 5. Views of incubated rMSCs (37 °C, 48 h, 4 mM G6.9F0.1C) using a) optical and b) fluorescence microscopy and c) their overlay. Scale bar 50 μm.

Fluorescence microscopy after a standard 48 h incubation of the cells in the presence of G6.9F0.1C showed a noticeable cellular uptake of the contrast agent (Figure 5).

The toxicity of these contrast agents was very low in the range of concentrations needed for sufficient labelling (1–4 mM of Gd^{III}). The cells grew slightly more slowly in the presence of the CAs (their number typically reached ~70–80% of that in a control experiment with unlabelled cells), with the fraction of living cells (measured after harvesting) reaching 85–95% (control experiments typically showed 95–98% viability under the same conditions). In the case of higher concentrations of CAs (8–16 mM of Gd^{III}), a noticeable fraction of cells became nonadherent and floating, and, very probably, the process of anoikis started, as revealed by a significant drop in the viability of the harvested cells to ~70%.[36] Such a process may be attributed to a large change in the osmolarity, as the GFC molecules are highly charged. In several tests, G5F2C was found to be slightly more toxic than G6.9F0.1C at higher Gd^{III} concentrations in the media (8–16 mM). Comparing these two CAs, the number of harvested cells was not markedly affected, but the viability was noticeably lower for the G5F2C agent. The higher toxicity of G5F2C can be attributed to the larger fluorescein content of the CA molecules, as it has been observed that high concentrations of fluorescein can be cytotoxic.[37]

Another crucial consideration with regard to the tracking of transplanted cells is the possible efflux of the internalized contrast agent out of the labelled cells.[38] Therefore, we performed a simple experiment to further examine the retention of the bimodal contrast agent in the labelled cells. rMSCs were labelled with G5F2C by the standard procedure. After 48 h, the medium containing the contrast agent was removed, the cells were washed twice with phosphate buffer, and new medium without contrast agent was added. The intensity of the fluorescence caused by the bimodal contrast agent in the cells was followed over a period of time using fluorescence microscopy. The results are shown in Figure 6. It was verified that our medium-sized conjugate was internalized in the cells. Even 24 h after labelling, the concentration of CA was still sufficient for cell visualization by fluorescence microscopy (however, some cells became nonadherent due to extensive manipulations within the well and, thus, the microscopic view was disturbed by floating cells; Figure 6d).

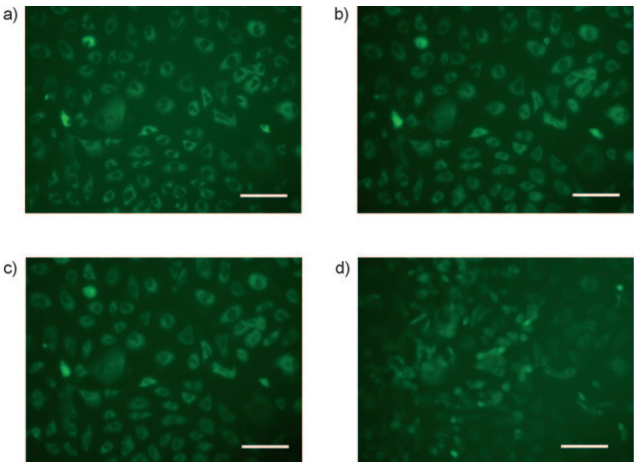

Figure 6. Photomicrographs of cell cultures labelled by G5F2C: a) cells after 48 h incubation at 37 °C in a medium containing 1 mM G5F2C, followed by a wash-out in phosphate buffer and the addition of new medium (without CA), $t=0$ h; b) at $t=1$ h of further cultivation; c) at $t=4$ h; d) at $t=24$ h. Scale bar 50 μm.

The relative stability of labelling of the stem cells by the GFC agents was confirmed by ICP-MS experiments. The cells were cultivated in a medium containing 1 mM Gd^{III} (as G6.9F0.1C) at 37 °C for 48 h. After this time, the cells were washed; one part was harvested, and the other was further cultivated in a GFC-free medium. These cells were harvested after 24 h of such a further cultivation. After mineralization, ICP-MS analyses revealed contents of 0.117 and 0.110 pg of Gd^{III} per cell, respectively, showing <10% efflux of the labelling agent (Table S2).

Conclusion

In summary, a novel bimodal fluorescence/MRI probe based on a cyclodextrin scaffold has been synthesized and characterized. The presence of several efficiently relaxing Gd^{III} centres within one molecule of moderate size leads to a high relaxivity of ~22 $s^{-1}mM^{-1}$ per Gd or ~150 $s^{-1}mM^{-1}$ per molecule of G6.9F0.1C (20 MHz, 25 °C) confined within a small molecular space (i.e., to a high density of relaxivity). This is especially useful in the field of cell imaging. A preliminary in vitro labelling of pancreatic islets and rat mesenchymal stem cells has been successfully performed. In spite of the

high charge of the complex, the agent G6.9F0.1C is not cytotoxic and is easily internalized into cells. An MRI phantom study revealed the efficient influence of a T_1 relaxation process, resulting in good detection of suspensions of labelled stem cells and individual pancreatic islets. It was found that incubation of cell cultures in media containing concentrations of GFC as low as 1 mM (per Gd^{III}) resulted in sufficient loadings for MRI visualization. A qualitative fluorescence study performed on mesenchymal stem cells showed that the CA stays in the intracellular space for a long time. Thus, tracking of the fate of labelled cells/PIs after transplantation using T_1-weighted MRI images might be possible. Preliminary experiments with labelled PIs have indicated the possibility of MRI visualization of transplanted cellular cultures even under in vivo conditions (rats).[39]

This work has confirmed that cyclodextrins are appropriate scaffolds for the production of high-relaxivity CAs and they are suitable, as nontoxic sugar derivatives, for cell labelling. This research is ongoing in our laboratories.

Experimental Section

General: All commercially available reagents and solvents were used as received. The ligand DO3AP^{NCS} (Figure 1)[25] and the per-6-amino-β-cyclodextrin core [$(NH_2)_7$-β-CD][23] were prepared according to published procedures. Fluorescein-isothiocyanate (FITC) was prepared from commercially available fluorescein-amine by the published procedure.[24] Gadolinium(III) chloride hydrate was obtained from Aldrich. Ultrafiltration equipment (UF-cell 8050 and 800 mL storage flask), including PLAC and PLBC membranes (Amicon, Bedford, MA), was purchased from Millipore. ^{1}H (400 MHz) and ^{31}P (161.9 MHz) NMR spectra were recorded on a Varian ^{UNITY}INOVA-400 spectrometer. NMR spectra were measured from samples in D_2O or [D_6]DMSO; chemical shifts are given in ppm referenced to *t*BuOH (D_2O) or residual protonated solvent ([D_6]DMSO) as internal references or to 85% H_3PO_4 as an external reference. Elemental analyses were carried out at the Institute of Macromolecular Chemistry (Academy of Sciences of the Czech Republic, Prague). Mass spectra were acquired on a Bruker ESQUIRE3000 ESI spectrometer in both positive- and negative-ion modes. UV/Vis spectra were measured on a Unicam UV300 UV/Vis spectrophotometer from solutions in 1.00 cm quartz cuvettes. Relaxivities were measured on a Bruker Minispec 20 relaxometer. The Gd^{III} content in labelled stem cells was determined by ICP/MS using a VG Elemental PQ3 spectrometer.

Synthesis of bimodal contrast agents (compounds GFC)

Synthesis of $(NH_2)_5$-F_2-β-CD: Per-6-amino-β-cyclodextrin hydrochloride [$(NH_2)_7$-β-CD·7 HCl·7 H_2O, 1.00 g, approx. 0.67 mmol] was dissolved in H_2O (2 mL), and the solution was adjusted to pH 7 with NaOH (0.106 g). DMSO (30 mL) was then added and the water was evaporated in vacuo. The resulting solution was mixed with a solution of FITC (0.52 g, 1.35 mmol) in DMSO (15 mL), and the mixture was stirred at RT for 2 days. The solvent was then evaporated using a Kugelrohr distillation apparatus. The crude solid product was dissolved in water (20 mL), the solution was adjusted to pH ≈ 10, and it was then continuously ultrafiltered through a PLAC membrane (1 kDa cut-off) at 3 atm until 500 mL of aqueous eluent had been collected. UV/Vis analysis of the remaining solution of the product and comparison thereof with the absorbance of the filtrate revealed that about 8% of the fluorescein (F) had been eluted (i.e., more than 90% of the fluorescein label remained bound to the cyclodextrin core). This gives an average statistical degree of substitution CD:F of around 1:2; therefore, this product is referred to as $(NH_2)_5$-F_2-β-CD in the following text. MS (negative): *m*/*z*: 1515.7 [$(NH_2)_6$-F-β-CD−H]$^-$, 1904.8 [$(NH_2)_5$-F_2-β-CD−H]$^-$; ^{1}H NMR ([D_6]DMSO): δ = 2.9–4.1 (br, 46 H; CD), 5.01 (br, 7 H; CD), 5.83 (br, 14 H; NH_2), 6.40–6.77 (br, 8 H; F), 7.13 (br, 4 H; F), 7.87 (br, 4 H; F), 8.53 ppm (br, 2 H; F). See also Figure S1.

Synthesis of L_5-F_2-β-CD: An aliquot of 80% of the previous product $(NH_2)_5$-F_2-β-CD (~0.54 mmol) was dissolved in H_2O (130 mL). The mixture was heated to 40 °C, and a solution of the bifunctional ligand DO3AP^{NCS} (L, pH 1–2), freshly prepared from DO3AP^{ABn} (5.00 g, 6.53 mmol),[5b] in H_2O (10 mL) was added in three portions over a period of 18 h. The mixture was re-adjusted to pH 9 after each addition using 2 M aqueous NaOH. The reaction mixture was then concentrated to a volume of 20 mL, and the solution was continuously ultrafiltered through a PLBC membrane (3 kDa cut-off) at 3 atm until 500 mL of aqueous eluent had been collected. The retenate was concentrated to dryness, affording 2.90 g of L_5-F_2-β-CD in the form of a non-stoichiometric sodium salt hydrate. ^{1}H NMR (D_2O): δ = 2.80–4.40 (br, 186 H; L + CD), 5.09 (br, 7 H; CD), 6.50 (br, 8 H; F), 6.8–8.1 ppm (br, 30 H; L + CD) (see also Figure S1); ^{31}P{^{1}H} NMR (D_2O): δ = 32.98 ppm (br s); elemental analysis: on the basis of the theoretical formula for the disubstituted product, $C_{199}N_{34}P_5S_7$, the relative amounts of these elements would be (%): 73.64/14.67/4.77/6.92; found: C 39.16, N 8.07, P 2.66, S 4.21, giving relative amounts (based on their sum being equal to 100%) of C/N/P/S (%): 72.39/14.92/4.92/7.78.

$(GdL)_5$-F_2-β-CD (compound G5F2C): A portion of the L_5-F_2-β-CD obtained above (2.70 g, 0.50 mmol) was dissolved in water (100 mL), and $GdCl_3$·6 H_2O (1.89 g, 5.07 mmol, ~10 molar equiv) was added. The mixture was adjusted to pH 7 with 2 M aqueous NaOH, and the resulting mixture was stirred overnight at 40 °C; some precipitation of $Gd(OH)_3$ occurred. After ~12 h, Na_2H_2EDTA (1.89 g, 5.07 mmol, 1 equiv per starting amount of Gd) was added and the mixture was re-adjusted to pH 7; during this process the precipitate completely dissolved. The solution was then ultrafiltered through a PLBC membrane (3 kDa cut-off) at 3 atm until 500 mL of aqueous eluent had been collected. The solvent was evaporated to yield 2.32 g of G5F2C as an orange glassy product. The Gd^{III} content was determined using a standard BMS experiment to be 0.64 mmol Gd^{III} per 1.00 g of the solid matter.

$(GdL)_{6.9}$-$F_{0.1}$-β-CD (compound G6.9F0.1C): This compound was prepared by a procedure analogous to that described above; however, an $(NH_2)_7$-β-CD to FITC molar ratio of 1:0.1 was used in the first reaction step. Although the isolated materials $(NH_2)_{6.9}$-$F_{0.1}$-β-CD and $L_{6.9}$-$F_{0.1}$-β-CD were highly coloured, it was not possible to obtain reliable ^{1}H NMR spectra confirming the presence of the fluorescein label in these molecules due to the very broad and un-integrable peaks of fluorescein in the aromatic region.

Comparison of MRI contrast efficiency of GFC with that of Gd–DOTA: Solutions of GFC and Gd–DOTA complexes (concentrations 0.1, 0.5, 1.0, and 2.0 mM) in water were sealed in 1 mm capillaries. These were stabbed into 35 mm diameter wells filled with 4% gelatine. MR measurements were performed using a 4.7 T (200 MHz) Bruker Biospec spectrometer equipped with a commercially available resonator coil (Bruker). A standard T_1-weighted CPMG multispin echo sequence (repetition time T_R = 730 ms, T_E = 14 ms, slice thickness = 0.7 mm, turbo factor = 2, number of acquisitions up to 128, FOV = 4 × 4 cm^2, matrix = 256 × 256) was used.

Cellular study: All protocols were approved by the Ethical Committee of the Institute for Clinical and Experimental Medicine, and the experiments were carried out in accordance with the European Communities Council Directive of 24 November 1986 (86/609/EEC).

MR relaxometry: The relaxivity was measured on a Minispec MQ20 (Bruker, Germany; 20 MHz, 25 °C).

MRI visualization of labelled pancreatic islets: Gel samples for imaging were prepared by placing 1–20 labelled pancreatic islets in a well (diameter 35 mm), in a single plane sandwiched between two layers of gelatine; the bottom layer was 4% gelatine and the top layer was 3% gelatine. MR measurements were performed using a 4.7 T Bruker Biospec spectrometer equipped with a commercially available resonator coil (Bruker) at 25 °C. A standard T_1-weighted CPMG multispin echo sequence (repetition time T_R = 219 ms, T_E = 14 ms, slice thickness = 0.63 mm, turbo factor = 2, number of acquisitions = 256, FOV = 4 × 4 cm^2, matrix = 256 × 256) was used.

MRI visualization of labelled stem cells: About 10^6 cells were labelled for 48 h as described above. After this time, the cells were harvested and counted in a Bürker chamber. The suspensions of the cells were transferred to 1 mm capillaries, which were sealed. The suspensions were left to settle by gravity for 24 h, and then the capillaries were stabbed into wells previously filled with 4% gelatine stabilized by 0.1% phenol and 0.1% NaN_3. MR measurements were performed using a 4.7 T Bruker Biospec spectrometer equipped with a commercially available resonator coil (Bruker) at 25 °C. A standard T_1-weighted CPMG multispin echo sequence (repetition time $T_R = 250$ ms, $T_E = 12$ ms, slice thickness = 0.63 mm, turbo factor = 1, number of acquisitions = 8, FOV = 4×4 cm^2, matrix = 256×256) was used.

Acknowledgements

Thanks are due to the Grant Agency of Charles University (2007-B-Ch-132307), the Academy of Science of the Czech Republic (No. KAN201110651), the Long-Term Research Plan of the Ministry of Education, Youth and Sports of the Czech Republic (No. MSM0021620857), the FP6 project DiMI (LSHB-CT-2005-512146) and EU FP7 project ENCITE (HEALTH-2007A-201842). Professor M. Mihaljevič is acknowledged for the ICP/MS measurements.

[1] a) M. Modo, M. Hoehn, J. W. M. Bulte, *Mol. Imaging* **2005**, *4*, 143–164; b) N. Muja, J. W. M. Bulte, *Progress NMR Spectrosc.* **2009**, *55*, 61–77.

[2] a) *The Chemistry of Contrast Agents in Medical Magnetic Resonance Imaging* (Eds.: A. E. Merbach, É. Tóth), Wiley, New York, **2001**; b) *Topics in Current Chemistry, Vol. 221*, Springer, Heidelberg, **2002**.

[3] a) P. Caravan, J. J. Ellison, T. J. McMurry, R. B. Lauffer, *Chem. Rev.* **1999**, *99*, 2293–2352; b) S. Aime, M. Botta, E. Terreno, *Adv. Inorg. Chem.* **2005**, *57*, 173–237; c) P. Hermann, J. Kotek, V. Kubíček, I. Lukeš, *Dalton Trans.* **2008**, 3027–3047; d) C. F. G. C. Geraldes, S. Laurent, *Contrast Media Mol. Imaging* **2009**, *4*, 1–23.

[4] D. H. Powell, O. M. N. Dhubhghaill, D. Pubanz, L. Helm, Y. S. Lebedev, W. Schlaepfer, A. E. Merbach, *J. Am. Chem. Soc.* **1996**, *118*, 9333–9346.

[5] a) J. Kotek, P. Lebdušková, P. Hermann, L. Vander Elst, R. N. Muller, C. F. G. C. Geraldes, T. Maschmeyer, I. Lukeš, J. A. Peters, *Chem. Eur. J.* **2003**, *9*, 5899–5915; b) J. Rudovský, J. Kotek, P. Hermann, I. Lukeš, V. Mainero, S. Aime, *Org. Biomol. Chem.* **2005**, *3*, 112–117; c) J. Rudovsky, P. Cígler, J. Kotek, P. Hermann, P. Vojtíšek, I. Lukeš, J. A. Peters, L. Vander Elst, R. N. Muller, *Chem. Eur. J.* **2005**, *11*, 2373–2384; d) P. Lebdušková, P. Hermann, L. Helm, É. Tóth, J. Kotek, K. Binnemans, J. Rudovský, I. Lukeš, A. E. Merbach, *Dalton Trans.* **2007**, 493–501.

[6] J. B. Livramento, A. Sour, A. Borel, A. E. Merbach, É. Tóth, *Chem. Eur. J.* **2006**, *12*, 989–1003.

[7] a) V. J. Venditto, A. I. S. Regino, M. V. Brechbiel, *Mol. Pharm.* **2005**, *2*, 302–311; b) S. Langereis, A. Dirksen, T. M. Hackeng, M. H. P. van Genderen, E. W. Meijer, *New J. Chem.* **2007**, *31*, 1152–1160.

[8] a) J. Rudovský, M. Botta, P. Hermann, K. I. Hardcastle, I. Lukeš, S. Aime, *Bioconjugate Chem.* **2006**, *17*, 975–987; b) P. Lebdušková, A. Sour, L. Helm, É. Tóth, J. Kotek, I. Lukeš, A. E. Merbach, *Dalton Trans.* **2006**, 3399–3406; c) Z. Jászberényi, L. Moriggi, P. Schmidt, C. Weidensteiner, R. Kneuer, A. E. Merbach, L. Helm, É. Tóth, *J. Biol. Inorg. Chem.* **2007**, *12*, 406–420; d) M. Polášek, P. Hermann, J. A. Peters, C. F. G. C. Geraldes, I. Lukeš, *Bioconjugate Chem.* **2009**, *20*, 2142–2153; e) D. T. Schühle, M. Polášek, I. Lukeš, T. Chauvin, É. Tóth, J. Schatz, U. Hanefeld, M. C. A. Stuart, J. A. Peters, *Dalton Trans.* **2010**, *39*, 185–191.

[9] a) S. Aime, A. Barge, C. Cabella, S. Geninatti Crich, E. Gianolio, *Curr. Pharm. Biotechnol.* **2004**, *5*, 509–518; b) S. Aime, S. Geninatti Crich, E. Gianolio, G. B. Giovenzana, L. Tei, E. Terreno, *Coord. Chem. Rev.* **2006**, *250*, 1562–1579; c) C. M. Long, J. W. M. Bulte, *Expert Opin. Biol. Ther.* **2009**, *9*, 293–306; d) W. Liu, J. A. Frank, *Eur. J. Radiol.* **2009**, *70*, 258–264.

[10] a) L. Frullano, T. J. Meade, *J. Biol. Inorg. Chem.* **2007**, *12*, 939–949; b) S. A. Corr, Y. P. Rakovich, Y. K. Gunko, *Nanoscale Res. Lett.* **2008**, *3*, 87–104; c) J. Kim, Y. Piao, T. Hyeon, *Chem. Soc. Rev.* **2009**, *38*, 372–390; d) S. Lee, X. Chen, *Mol. Imaging* **2009**, *8*, 87–100.

[11] L. E. Jennings, N. J. Long, *Chem. Commun.* **2009**, 3511–3524.

[12] a) M. J. Allen, T. J. Meade, *J. Biol. Inorg. Chem.* **2003**, *8*, 746–750; b) S. G. Crich, L. Biancone, V. Cantaluppi, D. D. G. Esposito, S. Russo, G. Camussi, S. Aime, *Magn. Reson. Med.* **2004**, *51*, 938–944.

[13] a) C. B. S. C. Morgan, A. S. Lowe, T. J. Meade, J. Price, S. C. R. Williams, M. Modo, *NMR Biomed.* **2007**, *20*, 77–89; b) J. Shen, X.-M. Zhong, X.-H. Duan, L.-N. Cheng, G.-B. Hong, X.-B. Bi, Y. Liu, *Acad. Radiol.* **2009**, *16*, 1142–1154.

[14] C. Cabella, S. Geninatti Crich, D. Corpillo, A. Barge, C. Ghirelli, E. Bruno, V. Lorusso, F. Uggeri, S. Aime, *Contrast Media Mol. Imaging* **2006**, *1*, 23–29.

[15] A. Mishra, J. Pfeuffer, R. Mishra, J. Engelmann, A. K. Mishra, K. Ugurbil, N. K. Logothetis, *Bioconjugate Chem.* **2006**, *17*, 773–780.

[16] T. Jin, Y. Yoshioka, F. Fujii, Y. Komai, J. Seki, A. Seiyama, *Chem. Commun.* **2008**, 5764–5766.

[17] Y. Song, X. Xu, K. W. MacRenaris, X.-Q. Zhang, C. A. Mirkin, T. J. Meade, *Angew. Chem.* **2009**, *121*, 9307–9311; *Angew. Chem. Int. Ed.* **2009**, *48*, 9143–9147.

[18] N. Kamaly, T. Kalber, G. Kenny, J. Bell, M. Jorgensen, A. Miller, *Org. Biomol. Chem.* **2010**, *8*, 201–211.

[19] a) W. Su, R. Mishra, J. Pfeuffer, K.-H. Wiesmüller, K. Ugurbil, J. Engelmann, *Contrast Media Mol. Imaging* **2007**, *2*, 42–49; b) A. Sturzu, M. Regenbogen, U. Klose, E. Echner, A. Gharabaghi, S. Heckl, *Eur. J. Pharm. Sci.* **2008**, *33*, 207–216; c) A. Sturzu, U. Klose, E. Echner, A. Beck, A. Gharabaghi, H. Kalbacher, S. Heckl, *Amino Acids* **2009**, *37*, 249–255.

[20] N. V. Evgenov, Z. Medarova, G. Dai, S. Bonner-Weir, A. Moore, *Nat. Med.* **2006**, *12*, 144–148.

[21] a) Y. Song, E. K. Kohlmeir, T. J. Meade, *J. Am. Chem. Soc.* **2008**, *130*, 6662–6663; b) J. M. Bryson, W.-J. Chu, J. H. Lee, T. M. Reineke, *Bioconjugate Chem.* **2008**, *19*, 1505–1509; c) J. L. Major, T. J. Meade, *Acc. Chem. Res.* **2009**, *42*, 893–903.

[22] M. Försterová, I. Svobodová, P. Lubal, P. Táborský, J. Kotek, P. Hermann, I. Lukeš, *Dalton Trans.* **2007**, 535–549.

[23] P. R. Ashton, R. Königer, J. F. Stoddart, D. Alker, V. D. Harding, *J. Org. Chem.* **1996**, *61*, 903–908.

[24] J. Pitra, V. Zoula, CS Patent 201892, **1980**.

[25] J. Rudovský, M. Botta, P. Hermann, A. Koridze, S. Aime, *Dalton Trans.* **2006**, 2323–2333.

[26] J. B. Livramento, É. Tóth, A. Sour, A. Borel, A. E. Merbach, R. Ruloff, *Angew. Chem.* **2005**, *117*, 1504–1508; *Angew. Chem. Int. Ed.* **2005**, *44*, 1480–1484.

[27] J. B. Livramento, C. Weidensteiner, M. I. M. Prata, P. R. Allegrini, C. F. G. C. Geraldes, L. Helm, R. Kneuer, A. E. Merbach, A. C. Santos, P. Schmidt, É. Tóth, *Contrast Media Mol. Imaging* **2006**, *1*, 30–39.

[28] S. Silvério, S. Torres, A. F. Martins, J. A. Martins, J. P. André, L. Helm, M. I. M. Prata, A. C. Santos, C. F. G. C. Geraldes, *Dalton Trans.* **2009**, 4656–4670.

[29] a) A. Hogan, A. Pileggi, C. Ricordi, *Front. Biosci.* **2008**, *13*, 1192–1205; b) V. Vaithilingam, G. Sundaram, B. E. Tuch, *Curr. Opin. Organ Transplant.* **2008**, *13*, 633–638.

[30] a) M. Woods, S. Zhang, A. D. Sherry, *Curr. Appl. Phys. Curr. Med. Chem. — Immunol. Endocrin. Metabol. Agents* **2004**, *4*, 349–369; b) A. Moore, *Eur. J. Radiol.* **2009**, *70*, 254–257; c) Z. Medarova, A. Moore, *Nat. Rev. Endocrin.* **2009**, *5*, 444–452.

[31] L. Biancone, S. Geninatti Crich, V. Cantaluppi, G. M. Romanazzi, S. Russo, E. Scalabrino, G. Esposito, F. Figliolini, S. Beltramo, P. C. Perin, G. P. Segoloni, S. Aime, G. Camussi, *NMR Biomed.* **2007**, *20*, 40–48.

[32] a) D. Jirák, J. Kříž, V. Herynek, B. Andersson, P. Girman, M. Burian, F. Saudek, M. Hájek, *Magn. Reson. Med.* **2004**, *52*, 1228–1233; b) J. H. Tai, P. Foster, A. Rosales, B. Feng, C. Hasilo, V. Marti-

nez, S. Ramadan, J. Snir, C. W. J. Melling, S. Dhanvantari, B. Rutt, D. J. G. White, *Diabetes* **2006**, *55*, 2931–2938.

[33] a) D. L. Kraichtman, W. D. Gilson, C. H. Lorenz, *J. Magn. Reson. Imaging* **2008**, *27*, 299–310; b) A. S. Arbab, J. A. Frank, *Regener. Med.* **2008**, *3*, 199–215.

[34] a) M. Hoehn, E. Kustermann, J. Blunk, D. Wiedermann, T. Trapp, S. Wecker, M. Focking, H. Arnold, J. Hescheler, B. K. Fleischmann, W. Schwindt, C. Buhrle, *Proc. Natl. Acad. Sci. USA* **2002**, *99*, 16267–16272; b) P. Jendelová, V. Herynek, J. DeCroos, K. Glogarova, B. Andersson, M. Hájek, E. Syková, *Magn. Reson. Med.* **2003**, *50*, 767–776; c) C. Bos, Y. Delmas, A. Desmouliere, A. Solanilla, O. Hauger, C. Grosset, I. Dubus, Z. Ivanovic, J. Rosenbaum, P. Charbord, C. Combe, J. W. M. Bulte, C. T. W. Moonen, J. Ripoche, N. Grenier, *Radiology* **2004**, *233*, 781–789; d) J. A. Frank, S. A. Anderson, H. Kalsih, E. K. Jordan, B. K. Lewis, G. T. Yocum, A. S. Arbab, *Cytotherapy* **2004**, *6*, 621–625; e) E. Syková, P. Jendelová, *Ann. N. Y. Acad. Sci.* **2005**, *1049*, 146–160; f) A. S. Arbab, G. T. Yocum, A. M. Rad, A. Y. Khakoo, V. Fellowes, E. J. Read, J. A. Frank, *NMR Biomed.* **2005**, *18*, 553–559; g) O. Hauger, E. E. Frost, R. van Heeswijk, C. Deminiere, R. Xue, Y. Delmas, C. Combe, C. T. W. Moonen, N. Grenier, J. W. M. Bulte, *Radiology* **2006**, *238*, 200–210; h) P. Walczak, J. Ruiz-Cabello, D. A. Kedziorek, A. A. Gilad, S. Lin, B. Barnett, L. Qin, H. Levitsky, J. W. M. Bulte, *Nanomedicine: Nanotechnol. Biol. Med.* **2006**, *2*, 89–94; i) E. Syková, P. Jendelová, *Prog. Brain Res.* **2007**, 161, 367–383; j) T. D. Henning, M. F. Wenland, D. Golovko, E. J. Sutton, B. Sennino, F. Malek, J. S. Bauer, D. M. McDonald, H. Daldrup-Link, *Magn. Reson. Med.* **2009**, *62*, 325–332.

[35] a) M. Rudelius, H. E. Daldrup-Link, U. Heinzmann, G. Piontek, M. Settles, T. M. Link, J. Schlegel, *Eur. J. Nucl. Med. Mol. Imaging* **2003**, *30*, 1038–1044; b) W.-C. Shyu, C.-P. Chen, S.-Z. Lin, Y.-J. Lee, H. Li, *Stroke* **2007**, *38*, 367–374.

[36] a) P. J. Reddig, R. L. Juliano, *Cancer Metastasis Rev.* **2005**, *24*, 425–439; b) J. E. Brinchmann, *J. Neurol. Sci.* **2008**, *265*, 127–130.

[37] S. Kato, S. Madachi-Yamamoto, Y. Hayashi, N. Miki, K. Negishi, *Brain Res.* **1983**, *313*, 143–147.

[38] P. J. Endres, K. W. MacRenaris, S. Vogt, T. J. Meade, *Bioconjugate Chem.* **2008**, *19*, 2049–2059.

[39] D. Jirák, V. Herynek, Z. Kotková, J. Kotek, M. Hájek, P. Hermann, I. Lukeš, unpublished results.

Received: December 22, 2009
Revised: April 15, 2010
Published online: June 25, 2010

